

Theoretical compressibilities of high-pressure ZnTe polymorphs

R. Franco, P. Mori-Sánchez, and J. M. Recio*

Departamento de Química Física y Analítica, Universidad de Oviedo, E-33006 Oviedo, Spain

R. Pandey

Physics Department, Michigan Technological University, Houghton, Michigan 49931, USA

(Received 12 June 2003; published 20 November 2003)

We report the results of a theoretical study of structural, electronic, and pressure-induced phase transition properties in ZnTe. Total energies of several high-pressure polymorphs are calculated using the density functional theory (DFT) formalism under the nonlocal approximation. Thermal effects are included by means of a nonempirical Debye-like model. In agreement with optical absorption data, the lowest direct gap of the zinc blende polymorph is found to follow a nonlinear pressure dependence that turns into linear behavior when expressed in terms of the decrease in the lattice parameter. The pressure stability ranges of cubic (zinc blende and rocksalt), trigonal (cinnabar), and orthorhombic (*Cmcm*) polymorphs are computed at static and room temperature conditions. Our calculations agree with the experimental and theoretical reported zinc blende \rightarrow cinnabar \rightarrow *Cmcm* pressure-induced phase sequence. Linear and bulk compressibilities are evaluated for the four polymorphs and reveal an anisotropic behavior of the cinnabar structure, which contrasts with the cubic-like compression of its shortest Zn-Te bonds. The qualitative trend shows a crystal that becomes relatively less compressible in the high-pressure phases.

DOI: 10.1103/PhysRevB.68.195208

PACS number(s): 64.60.-i, 71.15.Nc, 61.50.Ks, 61.50.Lt

Due to their technical and scientific importance, the structural and electronic behavior of II-VI compounds has been extensively investigated in the past decades. See, for example, Refs. 1 and 2 and references therein. Among the most interesting phenomena, the pressure-induced polymorphism is specially relevant, and demands theoretical and experimental studies to understand the observed changes including the semiconductor-metallic transformation exhibited by many II-VI materials under hydrostatic pressure. These first-order structural transitions increase the zero-pressure metal coordination in the lattice yielding a narrowing of the band gaps in these solids.

The study of compounds belonging to the ZnX ($X = \text{O, S, Se, Te}$) crystal family illustrates quite well how the identification and characterization of the polymorphic sequences have been performed. Besides the common wurtzite \rightarrow rocksalt (ZnO) and zinc blende \rightarrow rocksalt (ZnS) phase transitions, the high-pressure structures of ZnSe and ZnTe have been a matter of debate in the last decade.²⁻⁷ The x-ray diffraction experiments of Pellicer-Porres *et al.*³ allow us now to establish the existence of a (meta)stable cinnabar phase between the zinc blende and rocksalt structures in ZnSe. Conclusive experimental and theoretical results in ZnTe have recently confirmed the sequence zinc blende (ZnTe-I) \rightarrow cinnabar (ZnTe-II) \rightarrow *Cmcm* (ZnTe-III), although the presence of a rocksalt structure (ZnTe-IV) after ZnTe-III remains unclear.^{2,6,7} For ZnTe, static and room temperature phase diagrams, phase transition volumes, and structural parameters of the three phases are available. In addition, the nonlinear response under pressure of the lowest direct absorption gap of ZnTe-I (Refs. 8–10) have been also reported.

The compressibility changes along the polymorphic sequence in ZnX crystals have received less attention. In part, this is due to the short pressure range where the cinnabar

structure is found to be stable. On the other hand, the difficulty to obtain reliable equations of state (EOS) for phases not quenched at zero pressure prevents an accurate determination of the bulk modulus (B) of these high-pressure phases. Previous experimental (expt) and theoretical (theor) zero pressure B values (in GPa) are limited to the rocksalt structure of ZnO [194(expt), 170 ± 10 (theor) (Ref. 11)], ZnS [85.0(expt) (Ref. 12)], [82 ± 2 (theor) (Ref. 13)], and ZnSe [54 ± 2 (expt) (Ref. 3)]. As far as we know, neither experimental nor theoretical B_0 values have been reported for ZnTe-II, ZnTe-III, and ZnTe-IV phases.

Our work is directed to the evaluation of the crystal response to hydrostatic pressure of ZnTe polymorphs up to 20 GPa. The phase diagram is calculated at static and ambient conditions and is found to be in good agreement with pre-existent data. The observed pressure dependence of the ZnTe-I band gap is also obtained in our computations. Linear (bonding and lattice parameters) and bulk compressibilities are determined for the zinc blende, cinnabar, *Cmcm*, and rocksalt phases. The predicted trends are analyzed in terms of the increasing metal coordinations and Zn-Te bond lengths, and the more efficient packings of the high-pressure polymorphs.

The conventional unit cells of the four polymorphs belong to the $F\bar{4}3m$ (zinc blende), $P3_121$ (cinnabar), *Cmcm* (orthorhombic), and *Fm3m* (rocksalt) space groups. In our calculations, we have fixed the x and y fractional coordinates of Zn and Te in the cinnabar and orthorhombic phases, respectively, to the experimental values reported in Ref. 2. We have further checked that relaxation of these constrains decreases less than 10^{-4} hartree, the total energy of the polymorphs, although it was also detected that the difference between the x coordinates of Te and Zn in the cinnabar structure (Δx) becomes negligible. $\Delta x \sim 0$ has been observed in previous calculations⁷ and in the x-ray absorption experiments of San Miguel *et al.*⁴

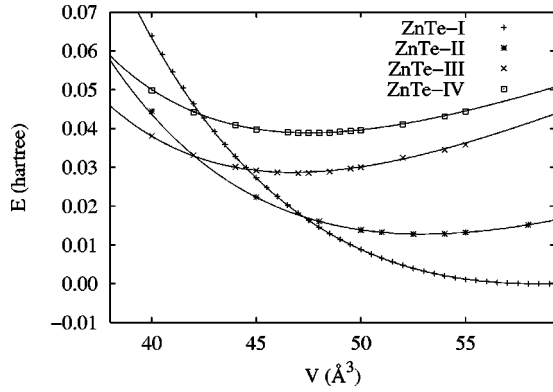


FIG. 1. Potential energy diagram for ZnTe-I (zinc blende), ZnTe-II (cinnabar), ZnTe-III (*Cmcm*), and ZnTe-IV (rocksalt) polymorphs. Energies (with respect to the value of the zinc blende structure at the equilibrium geometry) and volumes are per ZnTe unit formula. Symbols stand for the calculated values, whereas the curves are the fitting EOS.

The calculation of the electronic energy (E) at different volumes (V) of the several structures has been performed under the density functional theory (DFT), as implemented in the CRYSTAL package.¹⁵ Standard exchange and correlation density functionals from Becke¹⁶ and Perdew and Wang,^{17,18} respectively, have been included in the Kohn-Sham Hamiltonian. For Zn^{2+} , the basis set is the same as the one successfully used in earlier calculations on ZnO.¹⁹ For Te^{2-} , we have adopted an effective core pseudopotential,²⁰ while the valence space (including d -type polarization functions) has been reoptimized by minimizing the total energy of the zinc blende structure at the experimental equilibrium geometry.²¹ Based on previous experiences with the CRYSTAL code^{22,23} and after extensive computational tests, we decided to use the same basis sets for all the ZnTe phases explored in this work. It should be noted that our calculations differ from previous theoretical studies in the use of the gradient generalized approximation, in the inclusion of an all-electron basis set for Zn^{2+} , and in the consideration, as in the work of Lee and Ihm,⁶ of d -like orbitals in the active space of Te^{2-} .

The thermodynamic properties at finite temperatures have been calculated by means of a nonempirical quasiharmonic Debye model.²⁴ This model is based on the evaluation of the Debye temperature under the isotropic approximation and the estimation of the adiabatic bulk modulus by means of the static bulk modulus. This approach allows us to write all

thermodynamics quantities from the computed (E, V) points. To obtain the equilibrium volume at a given pressure (p) and temperature (T), we have invoked the thermodynamic equilibrium condition, namely, that the dynamic Gibbs energy is a minimum with respect to V . Isothermal EOS parameters are then obtained after analytical²⁵ and numerical fittings to the calculated $V(p; T)$ points.²⁶

The computed (E, V) values depicted in Fig. 1 contain the information concerning the static EOS and phase stability data of the four ZnTe polymorphs. It is apparent from these curves that the zero pressure density increases from ZnTe-I to ZnTe-III, the equilibrium volume of ZnTe-IV being slightly lower than that of ZnTe-III (see also Table I). In agreement with the observed sequence, the zinc blende phase is predicted to be the stable phase at $p=0$, whereas zinc blende \rightarrow cinnabar and cinnabar \rightarrow *Cmcm* phase transitions at increasing pressures are easily inferred from the existence of common tangents in the corresponding E - V curves. Therefore, we confirm that ZnTe is special among the II-VI semiconductors because the rocksalt is not a thermodynamical stable phase before the *Cmcm* structure. Two other interesting results are derived from this figure. First, the *Cmcm* \rightarrow rocksalt transformation is not possible according to our calculations. Second, a metastable rocksalt structure might be obtained directly from the zinc blende phase if we skip the cinnabar and *Cmcm* phases during the pressure load process. Details of the transition phase properties are given below.

As regards the characterization of these structures at zero pressure, the computed values collected in Table I provide, to the best of our knowledge, new detailed information for the high-pressure polymorphs, whereas for the zinc blende phase the comparison with the experimental data²⁸ is within the expected overestimation of the nonlocal density functional results. Inclusion of zero point vibrations and thermal effects at 300 K increase the lattice parameters roughly the same and about 0.8% in all the cases. It must be remarked that Lee and Ihm,⁶ and Côté *et al.*⁷ have previously optimized the unit cell geometry of ZnTe-II and ZnTe-III, but only numerical values are reported at high pressures.

Due to the intense interest and the existence of detailed experimental information in the zinc blende phase, it is also worthwhile to check and evaluate our computed band gap (E_g) energies at different pressures. The well known nonlinear response^{9,10,27} of E_g has been characterized by Strösser *et al.*⁹ using the following expression: $E_g(p) = 2.27$

TABLE I. Zero pressure equilibrium properties of ZnTe polymorphs according to our calculations. Experimental values from Ref. 28 in parentheses.

	ZnTe-I	ZnTe-II	ZnTe-III	ZnTe-IV
a (Å)	6.158 (6.1026)	4.305	5.655	5.749
b (Å)	6.158 (6.1026)	4.305	6.277	5.749
c (Å)	6.158 (6.1026)	9.899	5.267	5.749
V (Å ³)	58.39 (56.82)	52.96	46.75	47.51
B_0 (GPa)	47.7 (50.5)	51.4	62.2	57.0
B'_0	4.7 (5, fixed)	4.5	4.7	5.4

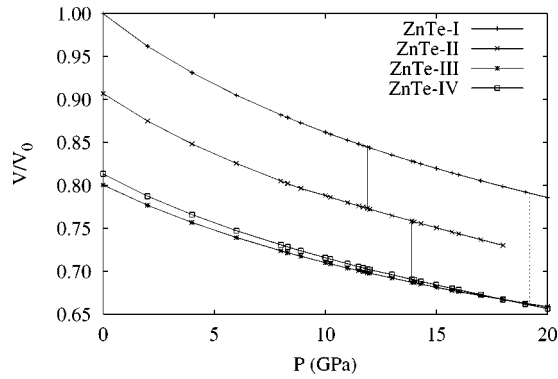


FIG. 2. Normalized volume-pressure diagram for ZnTe polymorphs. Vertical lines show the volume collapses at ZnTe-I \rightarrow ZnTe-II and ZnTe-II \rightarrow ZnTe-III phase transitions (solid lines), and the hypothetical ZnTe-I \rightarrow ZnTe-IV one (dotted line).

+0.104 p −0.0028 p^2 , where E_g is in eV and p goes up to 9.15 GPa. Our fitting in the 0–10 GPa range [$E_g(p)=2.46+0.109p-0.0022p^2$] shows a good agreement with the experimental function. When E_g is plotted against $-\Delta a/a_0$ (a is the unit cell lattice parameter and the zero subscript denotes $p=0$), the observed linear conduct allows us to distinguish the behavior of ZnTe-I from ZnSe-I, which is not possible with the $E_g(p)$ function.⁹ The corresponding calculated fitting gives a linear coefficient of 16.5 (16.2 in experiments), and a quadratic coefficient of 30.0, that accounts for a negligible deviation from the linear trend of our computed E_g versus $-\Delta a/a_0$ points.

Structural data for ZnTe-II and ZnTe-III have been also measured at selected pressures within the range where these phases have been found stable. After a number of resistivity,^{29,30} optical,⁹ x-ray absorption,⁴ and x-ray diffraction^{4,14} experiments, ZnTe-I \rightarrow ZnTe-II and ZnTe-II \rightarrow ZnTe-III transition pressures (p_{t1} and p_{t2}) are reported at 9.0 ± 0.5 and 12.0 ± 1.0 GPa, respectively. Our calculations yield $p_{t1}=11.9$ GPa and $p_{t2}=13.9$ GPa at static conditions, whereas $p_{t1}=12.0$ GPa and $p_{t2}=14.3$ GPa at 300 K, i.e., a small and negative change of the transition entropy is predicted. The overestimation in the computed p_t values may be traced back as due to the lack of global structural optimizations of the ZnTe-II and ZnTe-III unit cells, and the similar slopes of the $G(p)$ curves in the three polymorphs.⁶ In concordance with the above experiments, ZnTe-II is calculated to have a short stability pressure range of existence (around 2 GPa). Note also that the predicted slightly positive slope of the $p_t(T)$ curve agrees with the observed low sensitivity of the transition pressures to thermal effects up to room temperature. As pointed out above, the rocksalt phase is found to be metastable after a direct transformation from the ZnTe-I phase. The static and 300 K values for this transition are 19.2 and 19.3 GPa, respectively.

The volume reductions at the transition pressures are displayed in the V/V_0 - p diagram of Fig. 2. The computed $-\Delta V_t/V_0$ values are rather similar ($\sim 7.1\%$) for the ZnTe-I \rightarrow ZnTe-II and the ZnTe-II \rightarrow ZnTe-III transformations, whereas in the hypothetical ZnTe-I \rightarrow ZnTe-IV transition the volume collapse increases up to 13%. Zero-pressure data

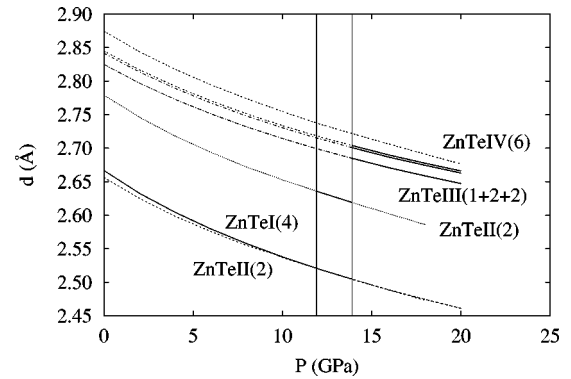


FIG. 3. Distance-pressure diagram of the shortest Zn-Te bonds in ZnTe polymorphs. Vertical lines separate pressure ranges where ZnTe-I, ZnTe-II, and ZnTe-III are the thermodynamically stable phases. Distances with solid lines belong to the stable phase in each pressure range. Numbers in brackets stand for the metal coordinations (see text).

give only slight overestimations of these transition volumes. The differences between $p=0$ and p_t values come from the decrease in compressibility in the higher-pressure phases, as the B_0 values collected in Table I reveal. San Miguel *et al.*⁴ found $-\Delta V_t/V_0$ to be also the same (13%) for the two observed transitions, though other experimental values² give higher values for ZnTe-I \rightarrow ZnTe-II ($\sim 9\%$) than for ZnTe-II \rightarrow ZnTe-III ($5.7\pm 2\%$). Assuming that our V/V_0 predictions are correct, this result suggests B_0 to be higher in ZnTe-III than in ZnTe-II, in agreement with our calculations. Theoretical $-\Delta V_t/V_0$ values from Lee and Ihm⁶ are 9% and 6%, while Côté *et al.*⁷ give 1.1% (too low) and 8.4% for the ZnTe-I \rightarrow ZnTe-II and the ZnTe-II \rightarrow ZnTe-III transitions, respectively. Although in Ref. 6 the ZnTe-II \rightarrow ZnTe-III phase transition is suggested to be “weakly first order,” all the above numbers point towards a reconstructive character of these structural transformations with atoms more closely packed in the higher-pressure structures.

The analysis of the atomic environments reveals different coordinations for Zn and Te in the less symmetric cinnabar and $Cmcm$ structures. In the zinc blende and rocksalt phases, both atoms display the same number of unlike nearest neighbors, 4 and 6, respectively. In the cinnabar phase, the fourfold coordination is kept (2+2) for Zn, but is 6 (3+3) for Te, whereas in the $Cmcm$ structure the number of Te and Zn unlike nearest neighbors is 5 (1+2+2). Therefore, a net increase in the effective coordination is seen along the ZnTe-I \rightarrow ZnTe-II \rightarrow ZnTe-III \rightarrow ZnTe-IV sequence. The numbers in parentheses stand for the number of atoms at different distances within a range of few tenths of Å (see below). According to the common behavior found in other reconstructive phase transformations, the increase in the coordination is accompanied by an increase in the bond lengths (see also Fig. 3). Thus, calculated Zn-Te distances in Å (experimental values in parentheses) are 2.666 (2.643) in ZnTe-I at 0 GPa, 2.538 (2.528) and 2.653 (2.646) in ZnTe-II at 9.6 GPa, and 2.700 (2.687), 2.715 (2.703), and 2.719 (2.706) in ZnTe-III at 11.5 GPa. The good theory-experiment agreement also supports reliability to our zero-pressure structural

data collected in Table I for the high-pressure phases of ZnTe.

We now look further into the compressibilities of the four polymorphs. The tendency in the calculated B_0 values shows lower compressible structures for the phases observed at higher pressures. The increase in B_0 from ZnTe-I to ZnTe-III is less than 30%. The rocksalt phase is predicted to compress slightly more than ZnTe-III (see also Fig. 2). We should emphasize at this point that, not only the B_0 values but also the trend in V_0 , suggest the rocksalt phase to behave as an intermediate structure between the cinnabar and $Cmcm$ polymorphs. In fact, the sequence zinc blende \rightarrow cinnabar \rightarrow rocksalt $\rightarrow Cmcm$ has been previously reported for CdTe.² Consistency to our results is also given by the fulfillment of the $B \sim 1/V$ empirical law³¹ since the calculated B_0V_0 products do not deviate appreciably from a constant value in the four polymorphs.

Linear compressibilities (κ_i , i is a lattice parameter or a bond length) have been also computed by means of a modified Vinet EOS.³² The quality of the fittings can be checked by the separate evaluation of the bulk compressibility (κ) from the inverse of B and from the thermodynamic relationship $\kappa = \kappa_a + \kappa_b + \kappa_c$. The pressure effects on the unit cell parameters of the cinnabar phase found the a axis to compress more than the c one ($\kappa_a = 7.19 \times 10^{-3} \text{ GPa}^{-1}$, $\kappa_c = 5.03 \times 10^{-3} \text{ GPa}^{-1}$) in agreement with the theoretical results of Côté *et al.*,⁷ but in contradiction with the slight decrease of the c/a ratio obtained in x-ray diffraction experiments,¹⁴ though only two values in a narrow pressure range of 2.6 GPa are reported. For CdTe, theoretical and

experimental results agree with our results for ZnTe, which seem to be reasonable due to the greater density of atoms along the helicoidal axis (c) of the cinnabar structure. In the orthorhombic phase, a quasi-isotropic behavior is obtained for the lattice parameter compressions.

Surprisingly enough, the bond compressibilities of the two shortest Zn-Te distances in the cinnabar phase are computed to be about the same (see Fig. 3). The value is also approximately equal to one-third of the bulk compressibility. The same result is obtained in ZnTe-III. Obviously, this relation also holds for the cubic phases. Two interesting conclusions can be derived. First, the lattice parameters in ZnTe-II accommodate their response against pressure to maintain a cubiclike compressibility for the bond lengths. Second, the bulk compressibility of the four polymorphs can be derived from the knowledge of the bonding compressibility. The global image we obtain is illustrated in Fig. 3 and reveals a somewhat striking behavior: the larger the Zn-Te distance, the lower the bond compressibility, the hypothetical rocksalt structure being again an exception. We, therefore, conclude that the decrease in the compressibility of the polymorphs observed at higher pressure originates not only from the increase in the effective atomic coordination, but also from the greater difficulty to compress the Zn-Te bonds.

Financial support from the Spanish DGICYT, Projects No. BQU2000-0466 and No. BQU2003-06553, are gratefully acknowledged. R.F. and P.M.S. also thank MCYT and the Fulbright Commission for grants.

*Corresponding author. Email address:

mateo@fluor.quimica.uniovi.es

¹M. L. Cohen and J. R. Chelikowsky, *Electronic Structure and Optical Properties of Semiconductors* (Springer, New York, 1989).

²R. J. Nelves and M. I. McMahon, in *Semiconductors and Semimetals*, edited by R.K. Willardson and E.R. Weber (Academic, New York, 1998), Vol. 54, p. 145.

³J. Pellicer-Porres, A. Segura, V. Muñoz, J. Zuñiga, J.P. Itié, A. Polian, and P. Munsch, *Phys. Rev. B* **65**, 012109 (2001).

⁴A. San Miguel, A. Polian, M. Gauthier, and J.P. Itié, *Phys. Rev. B* **48**, 8683 (1993).

⁵A. San Miguel, A. Polian, and J.P. Itié, *J. Phys. Chem. Solids* **56**, 555 (1995).

⁶G.-D. Lee and J. Ihm, *Phys. Rev. B* **53**, 7622 (1996).

⁷M. Côté, O. Zakharov, A. Rubio, and M.L. Cohen, *Phys. Rev. B* **55**, 13 025 (1997).

⁸N.E. Christensen and O.B. Christensen, *Phys. Rev. B* **33**, 4739 (1986).

⁹K. Strössner, S. Ves, C.K. Kim, and M. Cardona, *Solid State Commun.* **61**, 275 (1987).

¹⁰W. Walukiewicz, W. Shan, K.M. Yu, J.W. Ager III, E.E. Haller, I. Miotkowski, M.J. Seong, H. Alawadhi, and A.K. Ramdas, *Phys. Rev. Lett.* **85**, 1552 (2000).

¹¹J.M. Recio, M.A. Blanco, V. Luaña, R. Pandey, L. Gerward, and

J. Staun Olsen, *Phys. Rev. B* **58**, 8949 (1998).

¹²Y. Zhou, A.J. Campbell, and D.L. Heinz, *J. Phys. Chem. Solids* **52**, 821 (1991).

¹³J.M. Recio, R. Pandey, and V. Luaña, *Phys. Rev. B* **47**, 3401 (1993).

¹⁴R.J. Nelves, M.I. McMahon, N.G. Wright, and D.R. Allan, *Phys. Rev. Lett.* **73**, 1805 (1994).

¹⁵V. R. Saunders, R. Dovesi, C. Roetti, M. Causa, N.M. Harrison, R. Orlando, and C.M. Zicovich-Wilson, *CRYSTAL98 User's Manual* (University of Torino, Torino, 1998).

¹⁶A.D. Becke, *Phys. Rev. A* **38**, 3098 (1988).

¹⁷J.P. Perdew and Y. Wang, *Phys. Rev. B* **33**, 8800 (1986).

¹⁸J.P. Perdew and Y. Wang, *Phys. Rev. B* **40**, 3399 (1989).

¹⁹J. Jaffe and A.C. Hess, *Phys. Rev. B* **48**, 7903 (1993).

²⁰W.R. Wadt and P.J. Hay, *J. Chem. Phys.* **82**, 284 (1985).

²¹Details of the Te^{2-} basis set are available upon request.

²²R. Orlando, R. Dovesi, C. Roetti, and V.R. Saunders, *J. Phys.: Condens. Matter* **2**, 7769 (1993).

²³J. Jaffe, R. Pandey, and M.J. Seel, *Phys. Rev. B* **47**, 6299 (1993).

²⁴E. Francisco, J.M. Recio, M.A. Blanco, A. Martín Pendás, and A. Costales, *J. Phys. Chem. A* **102**, 1595 (1998).

²⁵P. Vinet, J.H. Rose, J. Ferrante, and J.R. Smith, *J. Phys.: Condens. Matter* **1**, 1941 (1989).

²⁶M. A. Blanco, E. Francisco, and J. M. Recio, GIBBS code (1997).

²⁷D.L. Camphausen, G.A.N. Connell, and W. Paul, *Phys. Rev. Lett.* **26**, 184 (1971).

- ²⁸L. Ley, A. Pollak, F.R. McFeely, S.P. Kowalczyk, and D.A. Shirley, *Phys. Rev. B* **9**, 600 (1974).
- ²⁹G.A. Samara and H.G. Drickamer, *J. Phys. Chem. Solids* **23**, 457 (1964).
- ³⁰A. Ohtani, M. Motobayashi, and A. Onodera, *Phys. Lett. A* **75A**, 435 (1980).
- ³¹R.M. Hazen and L.W. Finger, *J. Geophys. Res.* **84**, 6723 (1979).
- ³²E. Francisco, M.A. Blanco, and G. Sanjurjo, *Phys. Rev. B* **63**, 094107 (2001).